

Dynamical mean field theory of optical third harmonic generation

S. Akbar JAFARI^{1,2*}, Takami TOHYAMA¹ and Sadamichi MAEKAWA^{1,3}

¹ Institute for Materials Research, Tohoku University, Sendai 980-8577, Japan

² Department of Physics, Isfahan University of Technology, Isfahan 84156, Iran

³ CREST, Japan Science and Technology Agency, Kawaguchi 332-0012, Japan

(Received June 29, 2021)

We formulate the third harmonic generation (THG) within the dynamical mean field theory (DMFT) approximation of the Hubbard model. In the limit of large dimensions, where DMFT becomes exact, the vertex corrections to current vertices are identically zero, and hence the calculation of the THG spectrum reduces to a time-ordered convolution, followed by appropriate analytic continuation. We present the typical THG spectrum of the Hubbard model obtained by this method. Within our DMFT calculation, we observe a nontrivial approximate *scaling* function describing the THG spectra in all Mott insulators, independent of the gap magnitude.

KEYWORDS: Third harmonic generation, Mott insulator, Dynamical mean field

Nonlinear optical interactions of laser fields with matter provide powerful spectroscopic tools for the understanding of microscopic processes. The ability to control pulse durations (to a few femtoseconds), bandwidths (up to 1 Hz resolution), and peak intensities (up to 10^{19}W/cm^2) provides novel probes of elementary dynamic events of matter.¹

Observation of large third order nonlinear susceptibility in a quasi one dimensional Mott insulator Sr_2CuO_3 ($\chi^{(3)}$ values in the range 10^{-8} to 10^{-5} e.s.u.)^{4,5} poses the problem of nonlinear optical response in correlated insulators.

In systems with large on-site Coulomb interaction, the 1D system has the largest optical nonlinearity because of the decoupling of spin and charge degrees of freedom.^{6,7} On the other hand, mean field analysis shows that among SDW-ordered systems, the largest third order optical response appears in 2D.³ A natural generalization to higher dimensions is through the dynamical mean field theory (DMFT). DMFT includes the effect of local quantum fluctuations and becomes exact in the limit of infinite dimensions.

In this limit the self-energy becomes a purely local quantity determined from a self-consistent Anderson model. Then the matrix elements determining spectral weights are encoded in the local self-energy. In this limit the matrix element summations reduce to density of states (DOS) integrations. Therefore the combined DOS and self-energy effects give rise to nonlinear optical response of the system.

We formulate a nonlinear response theory, with example of THG within DMFT approximation and prescribe a numerically feasible method to avoid expensive computations. To our knowledge this is the first application of DMFT to nonlinear optics.

The general THG line shape within DMFT framework consists in a strong peak at three photon resonance, followed by a shoulder at two photon resonance, and a very weak feature at one photon resonance. The three-photon contributions obtained for various on-site Coulomb re-

pulsion fall approximately on the same curve, if we scale the frequencies with the gap magnitude. This behavior is similar to the one observed in band insulators,³ where a single particle picture describes the nonlinear optical processes.

We start with the Hubbard model at half filling

$$H = \frac{\tilde{t}}{\sqrt{d}} \sum_{\langle i,j \rangle, s} (c_{is}^\dagger c_{js} + \text{h.c.}) + U \sum_j \left(n_{j\uparrow} - \frac{1}{2} \right) \left(n_{j\downarrow} - \frac{1}{2} \right), \quad (1)$$

where c_{is}^\dagger creates an electron at site i with spin $s = \uparrow, \downarrow$. The dimension of the lattice is d . Here the $1/\sqrt{d}$ scaling of the hopping term ensures that average kinetic energy per particle in the limit of $d \rightarrow \infty$ remains finite.⁸

If we now imagine that we integrate out all degrees of freedom on various lattice sites, except for the one at the origin, we will be left with an effective action for this "impurity" site:

$$S_{\text{eff}} = - \int_0^\beta \int_0^\beta d\tau d\tau' \sum_\sigma c_{o\sigma}^\dagger(\tau) \mathcal{G}_o^{-1}(\tau - \tau') c_{o\sigma}(\tau') + U \int_0^\beta n_{o\uparrow}(\tau) n_{o\downarrow}(\tau). \quad (2)$$

Here the impurity propagator $\mathcal{G}_o(\tau - \tau')$ describes temporal quantum fluctuations between the four possible states of a single site at the origin, which must be determined self-consistently.

The simplest way to solve such effective impurity problem is the second order perturbation, which gives

$$\Sigma(\tau) = \frac{U^2}{4} \mathcal{G}_o(\tau) \mathcal{G}_o(\tau) \mathcal{G}_o(-\tau). \quad (3)$$

This gives the lattice Green's function as,

$$G(\vec{k}, i\omega_n) = 1/(i\omega_n - \varepsilon_{\vec{k}} - \Sigma(i\omega_n)). \quad (4)$$

The projection of this function on site 'o' is given by

$$G(i\omega_n) = \int \frac{D(\varepsilon) d\varepsilon}{i\omega_n - \varepsilon - \Sigma(i\omega_n)} \quad (5)$$

where $D(\varepsilon)$ is the lattice density of states. Finally the self-consistency between lattice (G) and impurity (\mathcal{G}_o) is

*E-mail address: akbar@imr.tohoku.ac.jp

via the Dyson equation

$$\mathcal{G}_o^{-1}(i\omega_n) = \Sigma(i\omega_n) + G^{-1}(i\omega_n), \quad (6)$$

which is used to update \mathcal{G}_o if the consistency has not been achieved yet.⁸

Solving the set of equations (3), (5) and (6) for various values of Hubbard U captures the physics of Mott metal-to-insulator transition.⁹ The essential many-body quantity provided by solving the local impurity problem is the self-energy which encodes the matrix element effects, as will be shown in the following. We solve¹⁰ the above set of equations at zero temperature for a Bethe lattice DOS of type $D(\varepsilon) = \frac{2}{\pi} \sqrt{1 - \varepsilon^2}$, which corresponds to renormalized hopping $\tilde{t} = t\sqrt{d} = 1/2$.

The third order nonlinear optical response per unit volume is related to four-current correlation $\chi_{jj}^{(3)}(\omega; \omega_1, \omega_2, \omega_3)$ by¹¹

$$\chi^{(3)}(\omega; \omega_1, \omega_2, \omega_3) = \frac{1}{3!} \left(\frac{-i}{\hbar} \right)^3 \frac{1}{V} \frac{\chi_{jj}^{(3)}(\omega; \omega_1, \omega_2, \omega_3)}{i\omega_n \omega_1 \omega_2 \omega_3}, \quad (7)$$

where $\omega = -\omega_\sigma = -(\omega_1 + \omega_2 + \omega_3)$, and the 4-current correlation function is given by

$$\chi_{jj}^{(3)}(\omega; \omega_1, \omega_2, \omega_3) = \int dx dx_1 dx_2 dx_3 e^{i\omega t + \omega_1 t_1 + \omega_2 t_2 + \omega_3 t_3} \times \langle T_c j(x) j(x_1) j(x_2) j(x_3) \rangle.$$

where $j(x)$ is current operator at space-time $x = (\vec{r}, t)$. Here T_c denotes the time-ordering along the Keldysh path.¹² Although the general formulation can be written down in terms of Keldysh Green's functions, but for parametric processes,² i.e. processes in which, final and initial states are identical, in practice one can avoid use of Keldysh Green's functions. In such a case one can use ordinary Green's function, to calculate the *time ordered* diagrams, followed by appropriate analytic continuation to ensure the correct $\nu + i\eta$ behavior of the fully retarded optical responses.³

The case of third harmonic generation corresponds to $\omega_1 = \omega_2 = \omega_3 = \nu$, so that we have

$$\chi^{\text{THG}}(\nu) \equiv \chi^{(3)}(-3\nu; \nu, \nu, \nu) = \frac{1}{18} \left(\frac{1}{\hbar} \right)^3 \frac{\langle \langle \langle \langle j j j j \rangle \rangle \rangle^{\text{THG}}(\nu)}{\nu^4}, \quad (8)$$

$$\langle \langle \langle \langle j j j j \rangle \rangle \rangle^{\text{THG}}(\nu) = \int dx e^{-3i\nu t} \Pi_i dx_i e^{i\nu t_i} \langle T j(t) j(x_1) j(x_2) j(x_3) \rangle.$$

The Feynman diagram corresponding to the THG process¹³ is shown in Fig. 1. In the limit of infinite dimensions vertex corrections to odd parity operators identically vanish by Ward identity. To see this, let us write down the Ward identity as¹⁴

$$-ik_\mu \Gamma^\mu(p+k, k) = G^{-1}(p+k) - G^{-1}(k) \quad (9)$$

where summation over $\mu = 0, 1, \dots, d$ is understood and p, k are $(d+1)$ -vectors. Using the Dyson equation the right hand side becomes $\Sigma(k+p) - \Sigma(k)$. In $d \rightarrow \infty$ limit self-energy is purely local⁸ (no k dependence) and hence it vanishes. Now, since the current (\propto velocity) vertex has odd parity under $\vec{k} \rightarrow -\vec{k}$, the vertex correction Γ^μ identically vanishes.

Therefore the four-current correlation $\langle \langle \langle \langle j j j j \rangle \rangle \rangle^{\text{THG}}(\nu)$ in Fig. 1 can be obtained by simple convolution. The

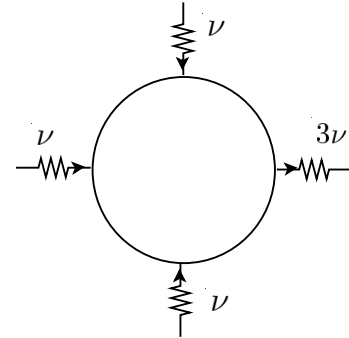


Fig. 1. Feynman diagram corresponding to the third harmonic generation. This diagram represents the *time-ordered* four-current correlation. To obtain the *fully retarded* four-current correlation we ensure the correct $\nu + i\eta$ analytic behavior.

Green's functions running around the loop are self-consistent lattice Green's function obtained from the impurity solver by iterated perturbation theory.⁸ Now let us further simplify $\langle \langle \langle \langle j j j j \rangle \rangle \rangle^{\text{THG}}(\nu)$ in $d \rightarrow \infty$ limit. Equation (8) can be written as

$$\chi^{\text{THG}}(i\nu) = \frac{1}{18} \frac{\langle \langle \langle \langle j_1 j_1 j_1 j_1 \rangle \rangle \rangle}{\nu^4} = \frac{8\tilde{t}^4}{9\nu^4} \frac{1}{Nd\beta} \sum_{\vec{k}, \omega_n} \sin^4(k_1) \times$$

$$G_{\vec{k}\sigma}(i\omega_n) G_{\vec{k}\sigma}(i\omega_n + i\nu) G_{\vec{k}\sigma}(i\omega_n + 2i\nu) G_{\vec{k}\sigma}(i\omega_n + 3i\nu)$$

where we have used the fact that current vertex in direction no. 1 is $2\tilde{t} \sin(k_1)$. To proceed further, we need to define $\rho_0(\varepsilon) = \frac{1}{Nd} \sum_{\vec{k}} \sin^4(k_1) \delta(\varepsilon - \varepsilon_{\vec{k}})$. To take the limit $d \rightarrow \infty$, we Fourier transform $\rho_0(\varepsilon)$ as:

$$\begin{aligned} \rho_0(s) &= \int \rho_0(\varepsilon) e^{is\varepsilon} d\varepsilon = \frac{1}{Nd} \sum_{\vec{k}} \sin^4(k_1) e^{is\varepsilon_{\vec{k}}} \\ &= \left[\int_{-\pi}^{\pi} e^{-2ist \cos k} \frac{dk}{2\pi} \right]^{d-1} \left[\int_{-\pi}^{\pi} \sin^4 k_1 e^{-2ist \cos k_1} \frac{dk_1}{2\pi} \right] \\ &= [J_0(2st)]^{d-1} \times \frac{1}{8} [3J_0(2st) - 4J_2(2st) + J_4(2st)] \\ &= \frac{1}{8} \left[3[J_0(2st)]^d + \mathcal{O}\left(\frac{1}{d}\right) \right], \end{aligned}$$

where J_n is the Bessel function of order n . In the last line we have used the fact that in $d \rightarrow \infty$ the hopping matrix element scales like $t = \tilde{t}/\sqrt{d}$ and hence $st \ll 1$, so that using $J_n(x) \approx \frac{x^n}{2^n n!}$, we can ignore J_2 and J_4 compared to J_0 . Repeating the above algebra without $\sin^4 k_1$ shows that, $[J_0(2st)]^d$ is indeed the Fourier transform of $D(\varepsilon)$. Therefore

$$\rho_0(\varepsilon) = \frac{3}{8} D(\varepsilon), \quad (10)$$

which allows us to write

$$\chi^{\text{THG}}(i\nu) = \frac{\tilde{t}^4}{3\nu^4 \beta} \sum_{\omega_n} \int d\varepsilon D(\varepsilon) \times \quad (11)$$

$$G(\varepsilon, i\omega_n) G(\varepsilon, i\omega_n + i\nu) G(\varepsilon, i\omega_n + 2i\nu) G(\varepsilon, i\omega_n + 3i\nu)$$

We see that in $d \rightarrow \infty$ the \vec{k} summation becomes simply a DOS integration. In the following ε stands for $\varepsilon_{\vec{k}}$, and the explicit ε subscript emphasises the \vec{k} label. From the

derivation it can be seen that other four current correlations like $\langle j_1 j_1 j_2 j_2 \rangle$ in $d \rightarrow \infty$ limit differ from $\langle j_1 j_1 j_1 j_1 \rangle$ by a numerical factor. Therefore to that extent the limit of $d \rightarrow \infty$ is blind to various directions in space. Hence DMFT can not distinguish optical spectroscopies with polarized light from those with unpolarized light.

To elucidate the matrix element effects in DMFT method, after Lehman representing the Greens' functions in terms of $A(\vec{k}, E) \rightarrow A(\varepsilon, E)$, and using standard contour integration techniques to perform $1/\beta \sum_{\omega_n}$ summation we obtain

$$\chi^{\text{THG}}(i\nu) = -\frac{\tilde{t}^4}{3\nu^4} \int d\varepsilon D(\varepsilon) dE_1 \dots dE_4 \quad (12)$$

$$A(\varepsilon, E_1) A(\varepsilon, E_2) A(\varepsilon, E_3) A(\varepsilon, E_4) \times F,$$

with

$$\begin{aligned} F = & \frac{f(E_1)}{E_1 - E_2 + i\nu} \frac{1}{E_1 - E_3 + 2i\nu} \frac{1}{E_1 - E_4 + 3i\nu} \\ & + \frac{f(E_2)}{E_2 - E_1 - i\nu} \frac{1}{E_2 - E_3 + i\nu} \frac{1}{E_2 - E_4 + 2i\nu} \\ & + \frac{f(E_3)}{E_3 - E_1 - 2i\nu} \frac{1}{E_3 - E_2 - i\nu} \frac{1}{E_3 - E_4 + i\nu} \\ & + \frac{f(E_4)}{E_4 - E_1 - 3i\nu} \frac{1}{E_4 - E_2 - 2i\nu} \frac{1}{E_4 - E_3 - i\nu} \end{aligned} \quad (13)$$

where f is the Fermi function. This expression closely resembles familiar expressions in nonlinear optics literature (see e.g. Sec. 3.2 of Ref. 2). Therefore in this formulation, the matrix element effects appear via spectral function $A(\varepsilon, E)$, which itself is fully determined by the self-energy. In principle after replacing $i\nu$ with $\nu + i0^+$ in this expression, we can use the spectral weights obtained from DMFT solver to calculate the nonlinear response. However, numerical calculation of the above five dimensional integrals is not computationally feasible.

Another alternative method would be to calculate χ^{THG} at Matsubara frequencies according to (11), followed by analytic continuation $i\nu \rightarrow \nu + i0^+$. But in this process, we face spurious features characteristic of analytic continuation of numbers, which makes it difficult to assess the nonlinear dynamical structures.

Since we are interested in high energy features in the scale of Mott gap, which is much larger than the thermal energies at room temperature, in order to avoid the above mentioned difficulties, we work at zero temperature. At $T = 0$, (11) will be replaced by

$$\chi^{\text{THG}}(\nu) = \frac{\tilde{t}^4}{6\pi\nu^4} \int d\omega d\varepsilon D(\varepsilon) \frac{1}{\xi_0 - \varepsilon} \frac{1}{\xi_1 - \varepsilon} \frac{1}{\xi_2 - \varepsilon} \frac{1}{\xi_3 - \varepsilon}, \quad (14)$$

where $\xi_j = \omega + j\nu - \Sigma_R(\omega + j\nu) + i|\Sigma_I(\omega + j\nu)|$ for $j = 0, 1, 2, 3$.

In the above formula, (i) the integration over ε corresponds to summation over intermediate states in conventional expressions² which are usually used for systems with discrete energy levels, and (ii) the matrix element effects are encoded in $\Sigma(\omega)$, real and imaginary part of which have been denoted by Σ_R and Σ_I , respectively. It is very crucial to note that we have used absolute value of the imaginary part of the self-energy. This is indeed

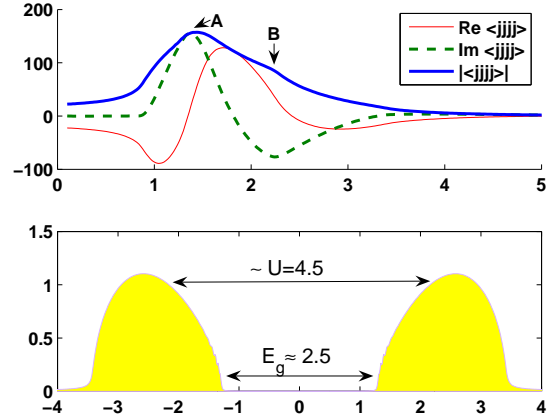


Fig. 2. (Color online) THG and DOS for $U = 4.5$. We use the Bethe lattice in solving DMFT equations. In the upper panel, dashed line is the imaginary part of $\langle jjjj \rangle$, narrow solid line represents its real part, and the bold solid line represents the absolute value. Lower panel shows the DOS. The onset of (3-photon) absorption at $\nu \approx 0.85$ corresponds to the gap value, $E_g \approx 2.5$, while peak-to-peak energy difference is on the scale of $U = 4.5$

a necessary step to transform from time-ordered four-current, to fully retarded one.³

Decomposing the integrand in (14) to partial fractions in terms of ε , the four-current correlation can be written as $f_0 + f_1 + f_2 + f_3$, where

$$f_j(\nu) = \frac{\tilde{t}^4}{6\pi} \int d\omega \prod_{s \neq j} \frac{1}{(\xi_j - \xi_s)} \int d\varepsilon \frac{D(\varepsilon)}{(\varepsilon - \xi_j)} \quad (15)$$

The expression (15) reveals the resonance structure transparently: It arises from $\omega + j\nu - \Sigma_R(\omega + j\nu) = \varepsilon$. When the frequency ν of the photons is such that j -photon frequency matches the energy difference $\varepsilon - \omega + \Sigma_R(\omega + j\nu)$, we will have a j -photon resonance. Here, f_0 corresponds to a background contribution.

Note that within this formulation, we do not have any control over the 'broadening' parameter η , instead the broadening $\eta = |\Sigma_I(\omega)|$ is determined by the solution of the impurity problem in a self-consistent fashion.

Now let us present our results. For semicircular Bethe lattice DOS of width $2\tilde{t} = 1$, the critical value is given by $U_c \approx 3.3$, above which system is in the Mott insulating state. Fig. 2 shows the result for $U = 4.5$. Lower panel shows the self-consistent DOS, with a Mott-Hubbard gap ~ 2.5 . The peak-to-peak separation between the upper and lower Hubbard bands is $\sim U = 4.5$. Upper panel shows real(dashed), imaginary(dotted) and absolute value(solid line) of the four-current correlation $\langle jjjj \rangle^{\text{THG}}$.

The onset of absorption starts at $\nu \approx 0.85$ which is $1/3$ of the gap magnitude. This can be clearly seen in the imaginary part of the THG four-current correlation in Fig. 2. This onset clearly corresponds to three-photon absorption. The three-photon resonance peaks around $\nu \approx 1.5$ (denoted by **A**) which is $1/3$ of the peak-to-peak separation of the Hubbard bands. Next weaker feature (denoted by **B**), which is a shoulder similar to finite-dimensional results,⁵ corresponds to $1/2$ of peak-to-peak separation (~ 4.5) of the Hubbard bands. The

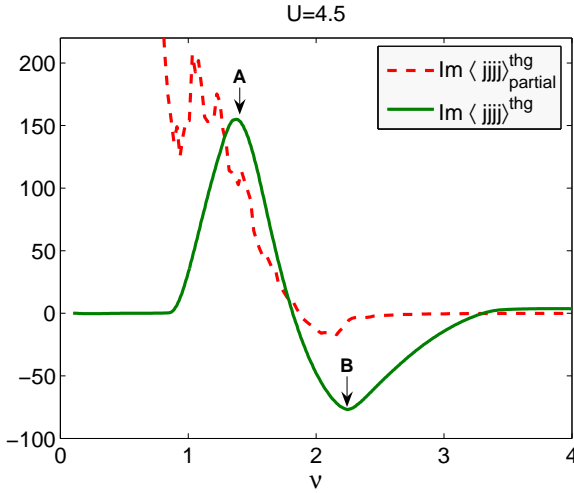


Fig. 3. Solid line shows the imaginary part of the total THG for $U = 4.5$. The dashed line shows the imaginary part of $f_3(\nu)$. **A** and **B** in this figure correspond to those in Fig. 2.

one-photon process is the weakest feature around $\nu \sim 4.5$ which can hardly be distinguished in THG spectrum. Despite that DMFT is designed to work better in larger dimensions, the spectrum in figure 2 qualitatively resembles the experimental result on Sr_2CuO_3 , which is a one-dimensional Mott insulator.⁵

We claimed that in peak **A** of Fig. 2 the dominant contribution comes from three-photon processes. To demonstrate this, in Fig. 3 we plot with dashed line, the imaginary part of $f_3(\nu)$. The solid line shows the total four-current correlation. As can be seen, the 3-photon resonance dominantly contributes to the peak **A**, although the peak position is slightly shifted to lower energies. Further, it is clearly seen that $f_3(\nu)$ does not contribute much to the two photon resonance at **B**. $f_3(\nu)$ also blows up at small frequencies which by (15) will be finally compensated by other partial spectra, f_0, f_1, f_2 , to give the total THG spectrum.

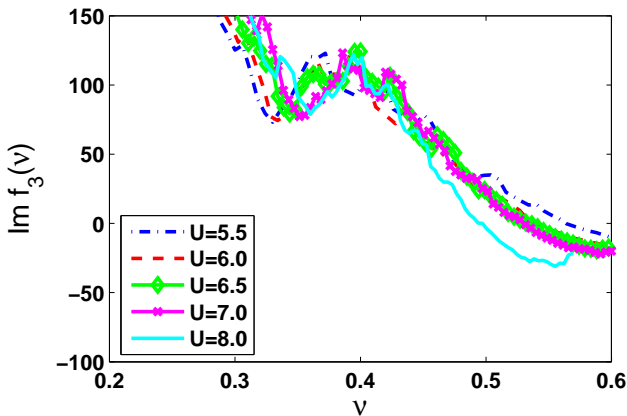


Fig. 4. Imaginary part of $f_3(\nu)$ vs. ν/E_g , where E_g is the Mott-Hubbard gap in the Mott insulating phase.

In our previous work,³ we found that within the SDW mean field the THG in e.g. 1D is given by $\Im\chi^{\text{THG}}(\nu) = \frac{27}{2}f(\frac{3\nu}{2}) - 8f(\nu) + \frac{1}{2}f(\frac{\nu}{2})$, in which

$$f(\nu) = \Delta \times \left[\frac{\pi}{24|\tilde{\nu}|^5} (\tilde{w}^2 - \tilde{\nu}^2)^{3/2} (\tilde{\nu}^2 - 1)^{1/2} \right] \quad (16)$$

where the gap $E_g = 2\Delta$, $\tilde{w}^2 = (1 + \Delta^2)/\Delta^2$, and the frequency $\tilde{\nu} = \frac{\nu}{\Delta}$ is scaled by the gap parameter. In the above equation $f(3\nu/2)$ corresponds to $f_3(\nu)$ defined in (15). We see that in the mean field approximation, $f_3(\nu)$ has a scaling part which is universal, and independent of the gap magnitude.

Motivated by this observation, in Fig. 4 we plot $\Im f_3$ for Mott insulators with various values of U as a function of $\frac{\nu}{E_g}$. We also apply an overall scaling to the curves. Such a scaling behavior, though approximate, points to a universal features in the nonlinear optical spectra of the Mott insulators, which are independent of the gap magnitude. It seems that the mean field scaling behavior survives the quantum fluctuations implemented via DMFT. It would be interesting to further explore this observation using alternative methods of dealing with correlated insulators.

In summary, on the technical side, we have formulated the nonlinear optical response theory within the DMFT theory. In equation (14) we present a feasible way that avoids numerical difficulties. On the physics side, assuming that DMFT is a good approximation for $d > 1$, we observe that nonlinear optical spectra of higher dimensional Mott insulators share common features with those observed in $d = 1$ dimensional Mott insulator, Sr_2CuO_3 .⁵ Also within DMFT we observe an approximate scaling behavior in the THG spectra of Mott insulators.

S.A.J. was supported by JSPS fellowship P04310. We wish to thank M.J. Rozenberg for using his code in solving DMFT equations. This work was supported by Grant-in-Aid for Scientific Research from the MEXT, and NAREGI project.

- 1) S. Mukamel, *Principles of Nonlinear Optical Spectroscopy*, Oxford University Press, 1995.
- 2) R. W. Boyd, *Nonlinear Optics*, 2nd Ed., Academic Press, 2003.
- 3) S.A. Jafari, T. Tohyama, and S. Maekawa, J. Phys. Soc. Jpn. **75** (2006) 054703.
- 4) H. Kishida, et al., Nature, **405** (2000) 929 and references therein.
- 5) H. Kishida, et al., Phys. Rev. Lett. **87** (2001) 177401.
- 6) Y. Mizuno, K. Tsutsui, T. Tohyama and S. Maekawa, Phys. Rev. B **62** (2000) R4769.
- 7) T. Tohyama and S. Maekawa, Jour. Lumi., **94-95** (2001) 659.
- 8) A. Georges, G. Kotliar, W. Krauth, and M.J. Rozenberg, Rev. Mod. Phys., **68** (1996) 13.
- 9) X.Y. Zhang, M.J. Rozenberg, and G. Kotliar, Phys. Rev. Lett., **70** (1993) 1666.
- 10) We use the code distributed by M.J. Rozenberg to participants in summer 2002 Trieste workshop on strongly correlated electron systems.
- 11) W. Wu, Phys. Rev. Lett. **61** (1988) 1119.
- 12) K. Chuo, Z. Su, B. Hao, and L. Yu, Phys. Rep., **118** (1985) 2.
- 13) J. Yu, and W.P. Su, Phys. Rev. B, **44** (1991) 13315.
- 14) M.E. Peskin, and D.V. Schroeder, *An Introduction to Quantum Field Theory*, Westview Press, 1995.